Radiative effect of ozone change on stratosphere-troposphere exchange

Fei Xie,[1] Wenshou Tian,[1,2] and Martyn P. Chipperfield[3]

[1] The potential radiative impact of ozone changes on stratosphere-troposphere exchange (STE) is investigated by a series of climate model simulations. The impact of an arbitrary 15% O_3 change on temperature, stratospheric water vapor, and cross-tropopause mass flux are compared to the corresponding effects from a doubling of atmospheric CO_2. Our analysis shows that a 15% global O_3 decrease can cause a maximum cooling of 2.4 K in the stratosphere and $\sim$7.2% increase in the tropical upwelling. This cooling also results in a higher tropical tropopause and lower tropopause temperatures, and hence less stratospheric water vapor and smaller amplitude of the so-called tape recorder signal. A global 15% O_3 increase gives rise to $\sim$2.1 K stratospheric warming and $\sim$4% decrease in the tropical upwelling. This O_3 increase results in more water vapor entering the stratosphere owing to a lower tropopause and higher tropopause temperatures. The effect of a $\pm$15% change in O_3 below 100 hPa is relatively small. However, the effect of a 15% O_3 increase between 200 and 70 hPa is similar to that of a 15% O_3 increase through the whole domain, suggesting that ozone increases in the UTLS dominate the impacts on temperature and tropical upwelling. Sea surface temperature (SST) changes associated with increasing atmospheric greenhouse gases (GHG) have a profound impact on the STE. Without corresponding SST changes, the radiative effects of the CO_2 doubling on the STE is less significant than a global 15% O_3 increase. When the SST changes are considered in the doubled CO_2 experiment, the tropical upwelling is significantly increased (by 20.4%) with a much higher, but warmer, tropopause.

Citation: Xie, F., W. Tian, and M. P. Chipperfield (2008), Radiative effect of ozone change on stratosphere-troposphere exchange, *J. Geophys. Res.*, *113*, D00B09, doi:10.1029/2008JD009829.

1. Introduction

[2] The Earth's climate is changing as a result of increasing GHGs in the atmosphere. The primary consequence of increased GHGs is to give rise to an overall warming of the troposphere and a cooling of the stratosphere, hence resulting in changes in the thermal structure of the atmosphere. These changes in the thermal structure have an important implication for stratosphere-troposphere exchange (STE) due to changes, among other things, in tropopause height and temperature, the intensity of wave activity and the strength of the Brewer-Dobson (BD) circulation [e.g., *Holton et al.*, 1995].

[3] Among the various GHGs, CO_2 is the most important and its impact on ozone recovery has been studied extensively [e.g., *Shindell et al.*, 1998; *Rosenfield et al.*, 2002]. Atmospheric ozone is not only photochemically active but is also radiatively important. Tropospheric ozone is a GHG while in the stratosphere ozone plays an important role in the shortwave and longwave radiation budget. Previous studies have shown that up to 30% of the surface and tropospheric warming resulting from GHG increases may have been offset by the cooling effect of stratospheric ozone loss during the period 1980 to 1999 [e.g., *Tett et al.*, 1996; *Roeckner and Stendel*, 1999; *World Meteorological Organization*, 1999].

[4] Since the discovery of the Antarctic ozone hole [*Farman et al.*, 1985], a negative trend in globally averaged total ozone column has been observed [e.g., *Intergovernmenal Panel on Climate Change*, 2001; *World Meteorological Organization*, 2003, 2007] while recent chemistry climate model (CCM) studies indicate that the ozone layer should tend to recover to 1980 values by around 2050 [*Eyring et al.*, 2007]. *Chipperfield and Feng* [2003] argued that CO_2-induced cooling may cause stratospheric O_3 to recover to values greater than 1980 levels during this century. Changes in atmospheric ozone not only give concern for human health due to its UV-attenuating effects, but also lead to climate changes both by direct radiative effects and indirectly by modifying dynamic processes in the atmosphere. It has been shown that the largest impact of ozone changes on climate occurs near the tropopause [e.g., *Forster and Shine*, 1997; *Hansen et al.*, 1997].

[1]College of Atmospheric Sciences, Lanzhou University, Lanzhou, China.

[2]Formerly at ICAS, School of Earth and Environment, University of Leeds, Leeds, UK.

[3]ICAS, School of Earth and Environment, University of Leeds, Leeds, UK.

Table 1. Ozone, CO_2 and SST Change Scenarios in Model Experiments

Experiment	Configuration
E1	Control experiment with no ozone change
E2	Global ozone decreased by 15%
E3	Ozone above 100 hPa decreased by 15%
E4	Ozone below 100 hPa increased by 15%
E5	Global ozone increased by 15%
E6	CO_2 concentration doubled
E7	CO_2 concentration doubled + Global ozone increased by 15%
E8	CO_2 concentration doubled + SST responses to $2 \times CO_2$
E9	Ozone between 200 hPa and 70 hPa increased by 15%

[5] There have been many studies on the climate effect of ozone changes using CCMs and general circulation models (GCMs) as well as simple radiative-convective models [e.g., *Ramanathan and Dickinson*, 1979; *Wang*, 1985; *Shindell et al.*, 1999, 2001; *Dameris et al.*, 2002; *Schwarzkopf and Ramaswamy*, 2002; *Karoly*, 2003; *Austin et al.*, 2003; *Chipperfield and Feng*, 2003; *Tian and Chipperfield*, 2005]. However, those studies mainly focused on ozone-induced temperature changes and related chemical feedbacks while less attention has been paid to the effect of ozone changes on STE processes. On the other hand, atmospheric ozone undergoes both chemical and radiative processes. In those CCM studies in which ozone is both chemically and radiatively coupled to the underlying GCM, it is hard to separate the radiative effects of ozone from chemistry-related effects. Until now, most CCMs have only included either tropospheric chemistry or stratospheric chemistry due to constraints of computer resources and the overall effect of ozone changes within the whole atmosphere has not yet been determined.

[6] In this paper, using a general circulation model (CAM3) which has been well tested in previous studies [e.g., *Collins et al.*, 2006; *Hurrell et al.*, 2006], we perform a series of time-slice runs to investigate potential impacts of ozone changes on STE processes. A change in ozone will feed back on temperature and, thus circulation through changing radiative heating rate and the temperature gradient. We will focus on the radiative-dynamic effect of ozone on STE processes; its chemical effect and associated feedbacks are not considered. Previous studies have shown that during the past several decades, global ozone has decreased by a factor of at least ~6% in the whole atmosphere and increased by 15% in the troposphere [e.g., *Johnson et al.*, 1999; *Randel et al.*, 1999; *Austin et al.*, 2003; *Collins et al.*, 2003; *Reinsel et al.*, 2005; *Stevenson et al.*, 2006; *Fioletov et al.*, 2006; *World Meteorological Organization*, 2007]. It is also likely that ozone in the whole atmosphere will increase by 6% by the end of this century owing to ozone recovery [e.g., *Eyring et al.*, 2007; *World Meteorological Organization*, 2007]. To understand the potential impact of ozone changes on STE and climate, we use different prescribed changes of ozone in the atmosphere. Climate responses to prescribed ozone changes are compared to corresponding responses caused by a doubling of atmospheric CO_2 in order to clarify the relative importance of

ozone changes. Section 2 gives a brief description of the model and numerical experiments. Section 3 presents the temperature and zonal wind responses to prescribed ozone changes while section 4 analyses the subsequent modulation of the BD circulation and cross-tropopause mass transport. Section 5 discusses the modulation of the water vapor entering from the troposphere to stratosphere due to these ozone changes and section 6 gives our summary.

2. Model Setup and Numerical Experiments

[7] The CAM3 model used in this study is a state-of-the-art 3D GCM provided by NCAR (http://www.ccsm.ucar.edu/models/atm-cam/). The model has a longitude-latitude resolution of $2.8° \times 2.8°$ with 26 levels extending from the surface to 4 hPa and a vertical resolution of about 2 km in the tropopause region. A general overview of CAM3 is given by *Collins et al.* [2004, 2006]. They showed that the model's radiation scheme performs well in simulating the radiative forcing of clouds and GHGs. *Boville et al.* [2006] showed that the CAM3 can simulate a relatively realistic tropopause and the common tropopause cold bias problem has been almost eliminated in the model (see also below).

[8] Nine time-slice runs have been performed for this study and the ozone change scenarios in each experiment are listed in Table 1. The GHG values used in the model radiation scheme are based on IPCC A2 scenario [*World Meteorological Organization*, 2003] 1990 values (CO_2, 353 ppmv; CH_4, 1.7 ppmv; N_2O, 308 ppbv; CFC11, 256 pptv; CFC12, 474 pptv). The sea surface temperatures (SST) used in experiments E1−E7 and E9 are observed monthly mean climatologies for the time period from 1949 to 2001 [*Rayner et al.*, 2003]. It should be noted that most previous studies on doubled CO_2 experiments have been performed with the SSTs also being altered to be consistent with the equilibrium response to doubled CO_2 in the atmosphere [e.g., *Rind et al.*, 1999, 2001; *Butchart et al.*, 2000, 2006]. In our experiments E1 to E7 and E9, the SSTs are all the same so that we can focus mainly on radiative effects of O_3 and CO_2 on STE. In experiment E8, the SST and sea ice fields were generated by UK Met Office Hadley Centre for the Chemistry-Climate Model Validation Activity (CCMVal) experiments described by *Eyring et al.* [2007]. The original data sets are monthly time series from 1980 to 2100. In E8, the 12-month climatology of the SST and sea ice fields for a doubled CO_2 atmosphere are calculated from the last 10 years of this data set, i.e., 2091−2100. The SSTs in E8 include the GHG-induced changes in the SST field so we can compare experiment E8 with the doubled CO_2 experiment without SST responses (E6). All experiments were ran for 16 years where the first 4 years are spin-up and only the remaining 12 years are used for the analysis. The model climatologies are based on the last 12 years of the model output except when otherwise stated.

[9] The ozone used in the model's radiation scheme is a monthly varying zonal mean climatology. Figure 1 shows the annual mean of this ozone climatology and the water vapor climatology from the control experiment E1. In order to verify that CAM3, a low top tropospheric GCM, can give a water vapor climatology near the tropopause region quantitatively consistent with those of full stratosphere GCMs, the water vapor field from a transient run (1978−
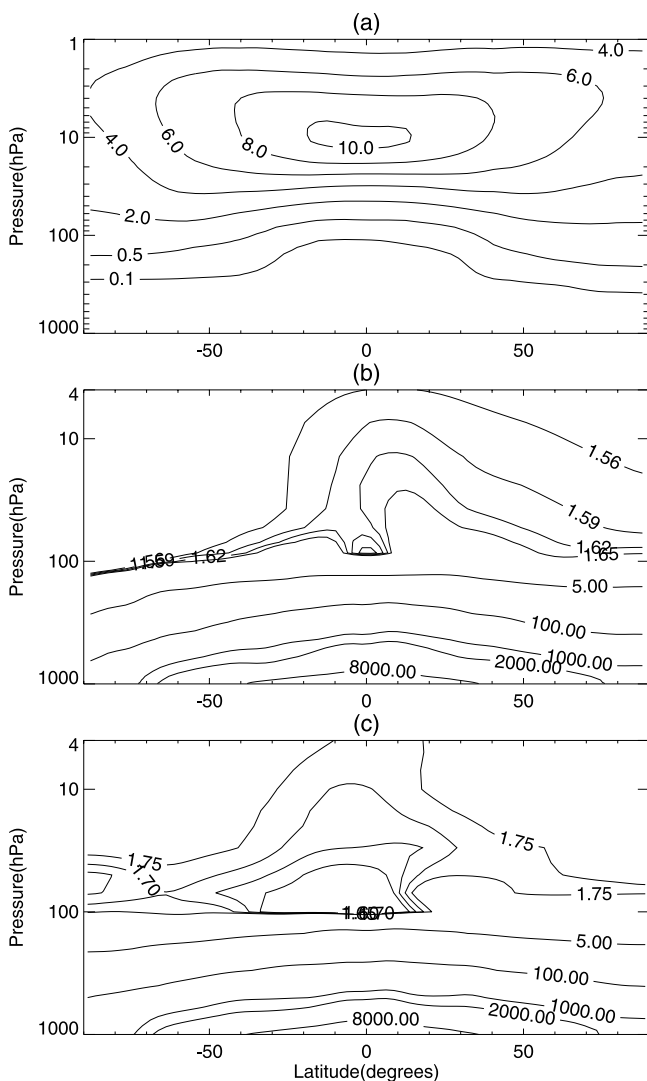
Figure 1. (a) Annual mean ozone climatology (ppmm) used in the model's radiation scheme. Also shown are water vapor climatologies (ppmv) from (b) the control experiment E1 and (c) an experiment simulates from 1978 to 2019 of the U.K. Met Office UM (64-level version).

2019) of the UK Met Office Unified Model (UM) (64-level version) is analyzed. The water vapor climatology for the period of 1980–2000 (approximately a 1990s climatology) from this transient run is also shown in Figure 1. More details of this UM experiment is given by *Tian and Chipperfield* [2006]. Note that water vapor climatologies from both the CAM3 and UM are much lower than observed values in the stratosphere owing to the absence of methane oxidation. It should be noted that an unrealistic stratospheric water vapor climatology will cause biases in radiation fluxes in the stratosphere. However, all results in this study are interpreted from differences between two model climatologies and the net effect of those biases on the results of this paper should be small. On the other hand, *Tian and Chipperfield* [2006] found from a CCM that water vapor in the lower stratosphere is largely related to changes in temperature and transport near the tropopause. Figure 1

also indicates that in the upper troposphere and lower stratosphere (UTLS) region, the magnitudes of water vapor in both models are similar.

[10] Figure 2 shows the modeled temperature and westerly wind climatologies from the control experiment E1 and the UM run mentioned above. Also shown are the corresponding temperature and westerly wind climatologies for the time period from 1984 to 1993 from National Centers for Environmental Prediction (NCEP) reanalysis (http://www.sparc.sunysb.edu/html/model_index.html). We can see that the modeled temperature climatology compares well with NCEP reanalysis and the UM output. However, the westerly jet in CAM3 is too strong compared to those of the NCEP and UM climatologies, possibly owing to effects of the low model top and the crude gravity wave drag scheme in CAM3.

3. Temperature and Circulation Responses to Ozone Changes

[11] Atmospheric ozone absorbs ultraviolet and infrared radiation so changes in O_3 concentrations will directly influence atmospheric temperature through radiative processes. Figure 3 shows responses of the temperature field to prescribed ozone changes in different experiments. A global 15% ozone decrease causes a significant cooling in the stratosphere with a maximum 2.4 K decrease in the middle stratosphere (Figure 3a). This cooling is proportionally in accordance with CCM predictions [e.g., *Tian and Chipperfield*, 2005]. *Wang* [1985] used a one-dimensional model and demonstrated that a 15% decrease in the middle stratospheric ozone can even cause a maximum 4 K temperature decrease. The temperature changes in the middle and lower troposphere caused by a global 15% ozone decrease are not significant at 95% confidence. However, in the tropics, statistically significant cooling can be noted down to the middle troposphere. Here the statistical significance is estimated by Student's T-statistic which tests whether two sample populations have significantly different means. Compared to experiment E3, in which ozone concentrations above 100 hPa are reduced by 15% (Figure 3b), the cooling in Figure 3a is slightly smaller than that in Figure 3b in the middle stratosphere in the tropics and midlatitudes. A comparison of Figures 3a and 3b reveals that although the decrease of ozone below 100 hPa gives no statistically significant temperature difference in most of the troposphere, it has an impact on stratospheric temperatures. Figures 3a and 3b also indicate that the statistically significant cooling in the middle and upper troposphere in Figure 3a is not a consequence of the decrease in ozone below 100 hPa.

[12] Figure 3c indicates that a 15% increase in ozone below 100 hPa nearly causes no significant temperature response in the troposphere. However, it leads to a cooling of about 0.3 K at high southern latitudes and 1.2 K at high northern latitudes in the middle stratosphere. This result is in accordance with Figures 3a and 3b and implies that a decrease of ozone below 100 hPa tends to cause a warming in the middle stratosphere. The underlying mechanism for this stratosphere-troposphere interaction may be related to stratospheric water vapor changes caused by ozone changes which are discussed in detail in section 5.
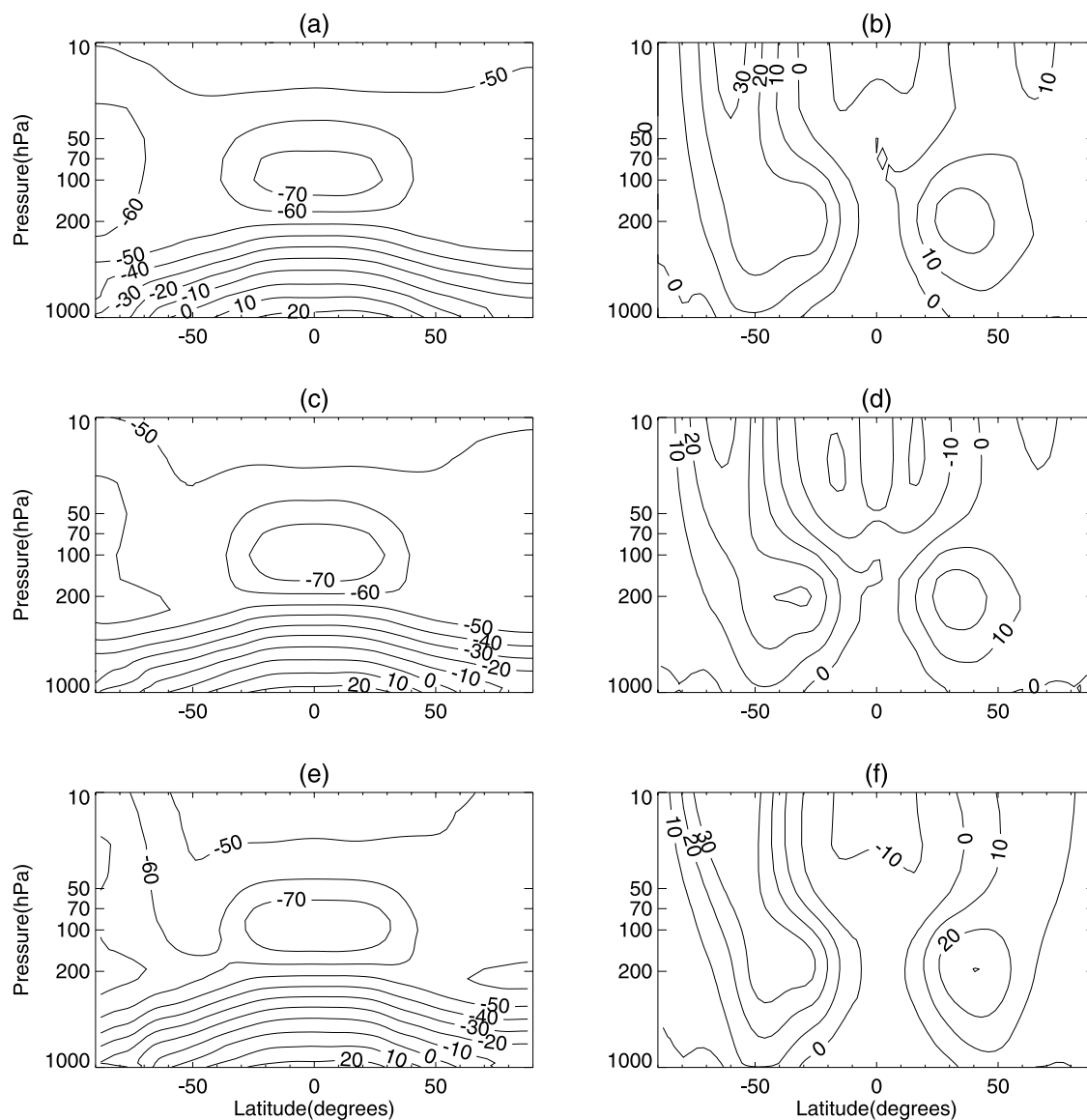
Figure 2. Latitude-pressure cross sections of zonal mean climatologies of temperature and zonal wind from (a, b) the NCEP reanalysis data for the time period from 1984 to 1993, (c, d) a 40-year experiment of the 64-level UM from UK Met Office, and (e, f) the control experiment E1. Contour intervals are 10 K for the temperature and 10 m s^{-1} for zonal wind.

[13] A global 15% ozone increase results in global temperature increases (Figure 3d) with a maximum warming of 2.1 K in the middle stratosphere. Statistically significant warming regions in Figure 3d extend farther downward compared to the cooling regions in Figure 3a. As expected, the doubling of CO_2 causes significant cooling in the stratosphere which is about three times as large as that caused by a 15% decrease of ozone above 100 hPa (Figure 3e). A question that arises here is what are the temperature responses to an ozone change in a doubled-CO_2 atmosphere? Figure 3f shows temperature responses to a CO_2 doubling and a global 15% O_3 increase. The integrated effect of these cause more significant warming in the troposphere and less cooling in the stratosphere compared to the doubled CO_2 experiment (Figure 3e). Also noticeable in Figure 3f is a pronounced warming in the tropical UTLS region where the warming is not significant in the doubled

CO_2 experiment. A 15% O_3 increase in the UTLS region causes a maximum warming of 1.2 K in the tropopause region (Figure 3h). This warming of tropopause allows more water vapor to enter the stratosphere causing a cooling (0.2 ∼ 1.0 K) in the high-latitudes stratosphere. Comparing Figures 3f and 3h, we can see that in the UTLS the 2xCO_2-induced warming is quite similar compared to the warming from a 15% O_3 increase in the UTLS region.

[14] Note that experiments E1 to E7 do not account for the SST responses to CO_2 doubling and O_3 changes. When SSTs are altered to include the equilibrium response to changing GHGs in the atmosphere, the temperature response to increased GHGs is different. Figure 3g shows the temperature differences between experiment E8 and E1. Compared to Figure 3e, we can see that the warming in the troposphere is significantly enhanced when the SSTs are changed. Figure 3h indicates that a 15% increase of ozone
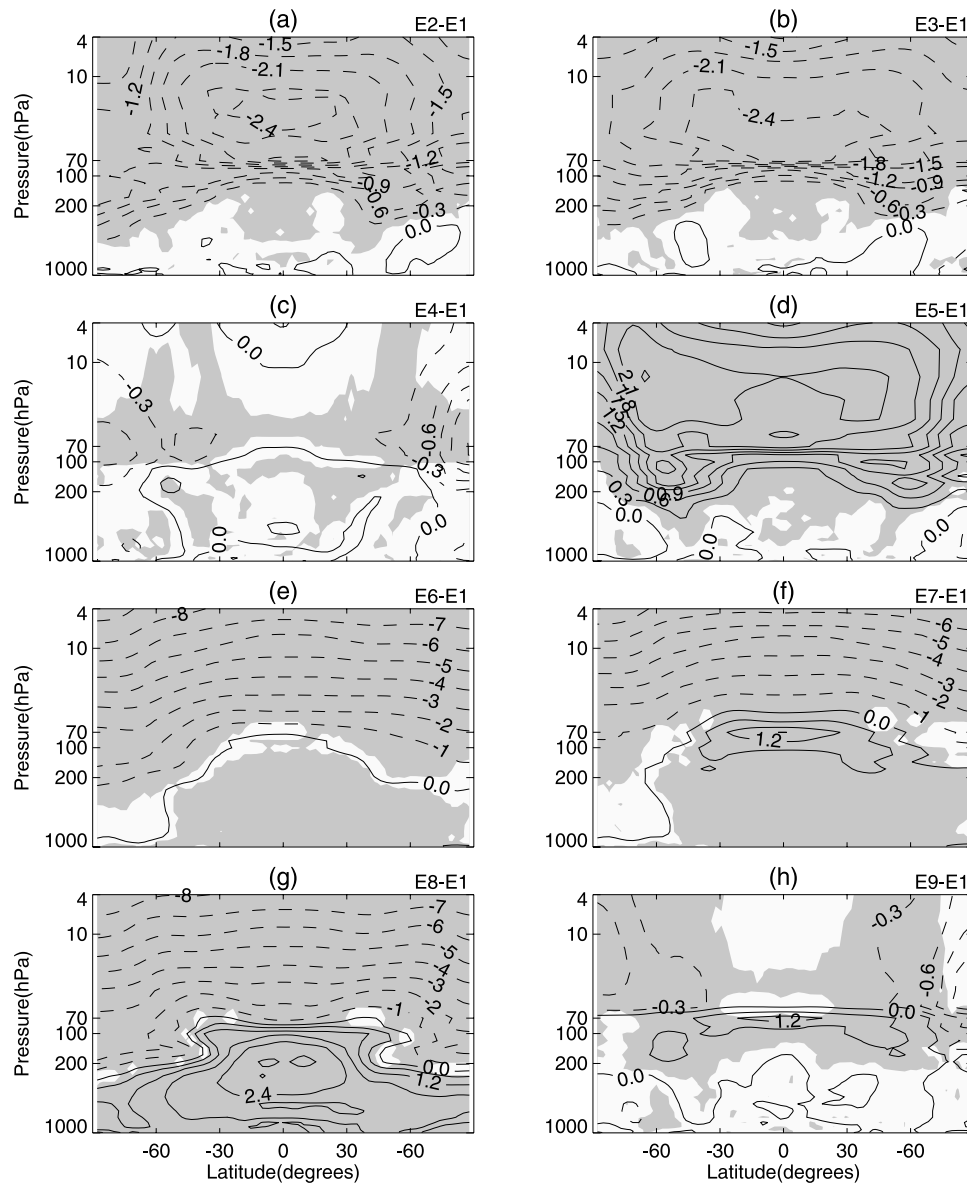
Figure 3. Latitude-pressure cross sections of zonal mean temperature differences (K) between experiments (a) E2 and E1, (b) E3 and E1, (c) E4 and E1, (d) E5 and E1, (e) E6 and E1, (f) E7 and E1, (g) E8 and E1, and (h) E9 and E1. Differences significant at 95% confidence level are shaded. Solid lines represent positive values, and dashed lines represent negative values.

between 200 and 70 hPa causes a 1.2 K warming in the UTLS region. Statistically significant cooling can also be noted in the stratospheric higher latitudes, which may be due to water vapor changes caused by the ozone increases between 100 and 70 hPa.

[15] Figure 4a further shows the temperature differences between experiments E7 and E6. Comparing Figure 4a with Figure 3d shows that temperature responses to a global 15% O_3 increase in a doubled CO_2 atmosphere are overall the same as those in experiment E5. However, at middle to high latitudes, temperature responses to a 15% O_3 increase in a $2\times CO_2$ atmosphere are slightly different from those in a $1\times CO_2$ atmosphere, as can be seen from Figure 4b. The warming of polar regions due to a 15% O_3 increase in a doubled CO_2 atmosphere (E7-E6) is more significant than in a $1\times CO_2$ atmosphere (E5-E1).

[16] Figure 5 shows the latitude-pressure cross sections of zonal mean zonal wind differences for experiments E5 to E8 relative to the control experiment E1. Differences in the zonal wind caused by a 15% global ozone decrease (E2), a 15% decrease in ozone above 100 hPa (**E3**), a 15% increase in ozone below 100 hPa (E4) or a 15% ozone increase between 200 and 70 hPa (E9) exhibit no consistent patterns of statistical significance (not shown). It appears that the tropospheric cooling caused by ozone decreases does not generate significant responses in the stratosphere. However, a global 15% ozone increase causes statistically significant differences in the zonal wind in stratosphere at lower latitudes and southern high latitudes (Figure 5a). The warming due to a 15% global O_3 increase gives rise to stronger westerly winds over polar regions but weaker westerlies in the midlatitude stratosphere. Zonal wind differ-
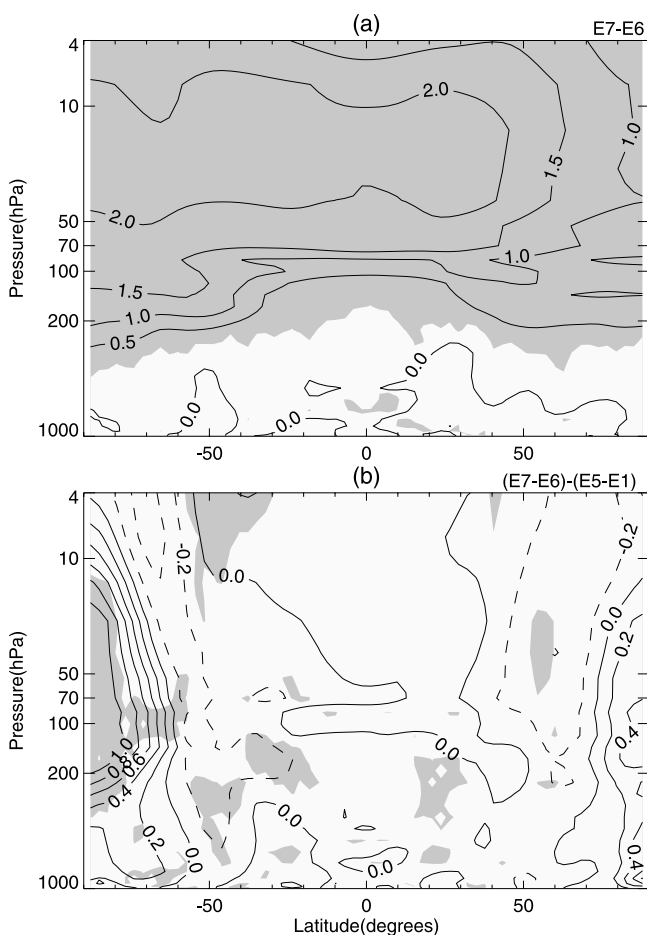
Figure 4. Zonal mean temperature differences (K) between (a) experiment E7 and E6. (b) Zonal mean temperature differences calculated from (E7-E6) − (E5-E1). Differences significant at 95% confidence level are shaded. Solid lines represent positive values, and dashed lines represent negative values.

ences in the tropical upper stratosphere are also strengthened by a 15% O_3 increase. The results here suggest that the warming of the stratosphere and upper troposphere due to a global ozone increase tends to strengthen the polar vortex but weaken the middle latitude westerly jet. In contrast, in doubled CO_2 experiment E6 the significant cooling effect in the stratosphere tends to accelerate westerly winds in the southern hemisphere midlatitude stratosphere (Figure 5b). Previous studies have shown that increasing greenhouse gases tend to cool the polar stratosphere, and to warm the tropical upper troposphere. Consequently, this increases the meridional temperature gradient in the tropopause region and the stratospheric zonal wind via the thermal wind relationship. *Shindell et al.* [2001] pointed out that this could also strengthen the polar vortex through the wave-mean flow mechanism. It is obvious from Figures 5a and 5b that circulation responses to a global ozone increase are different to those from a CO_2 doubling.

[17] By looking at Figures 5a, 5b and 5c together, we can note that a global 15% ozone increase (**E5**) and 2xCO_2 have a reversed effect on circulation, particularly in the southern and tropical stratosphere. From Figure 5d we can see that

circulation changes in experiment E8 (2xCO_2 + SST change) are much larger than those in the other experiments with significant acceleration of westerlies at high latitudes and weakening of zonal wind in the tropical stratosphere. It is apparent that a 15% increase of atmospheric ozone has a more significant impact on circulation than a 15% decrease, while the effect of a global 15% ozone increase on circulation is as significant as that of CO_2 doubling if the SST responses to CO_2 doubling are not considered.

4. Effect of Ozone Changes on Global Mass Flux

[18] Previous studies have shown that increasing GHGs tend to increase the mass exchange between the stratosphere and troposphere owing to a strengthened BD circulation [e.g., *Rind et al.*, 2001; *Butchart and Scaife*, 2001; *Butchart et al.*, 2006]. The results from those previous studies indicate that a doubling of CO_2 can cause substantial increase in the mass exchange across the tropopause. It is still unclear to what extent the changing atmospheric ozone modifies and affects the cross tropopause mass exchange. It is well known that the BD circulation, which consists of a vertical and a meridional component of the stratospheric motion, plays an important role in the mass exchange between stratosphere and troposphere. It is necessary here to examine first the potential impact on ozone changes on the BD circulation. The formulae to calculate the BD circulation in a pressure coordinate system are given by *Edmon et al.* [1980, 1981]

$$\vec{v}' = \bar{v} - \left[\left(\overline{v'\theta'} \right) / \bar{\theta}_p \right]_p$$

$$\bar{\omega}' = \bar{\omega} + (a\cos\phi)^{-1} \left[\cos\phi \left(\left(\overline{v'\theta'} \right) / \bar{\theta}_p \right) \right]_\phi,$$

where θ is the potential temperature, a is the radius of the earth, $\bar{v}$ is mean meridional wind, $\bar{\omega}$ is mean vertical velocity in pressure coordinates. Subscripts p and ϕ denote derivatives with pressure p and latitude ϕ, respectively. The overbar denotes the zonal mean and the accent denotes the deviations from the zonal mean value.

[19] The diagnosed BD circulation, EP flux vectors and annual cycle of the vertical velocity of the BD circulation in the control experiment E1 are shown in Figure 6. We can see that the model gives a reasonable pattern of the circulation with strong upwelling from the tropical troposphere to stratosphere and downwelling in the middle and high latitudes. The EP flux vectors and the annual cycle of the vertical velocity of the BD circulation are in accordance with those in previous studies [e.g., *Butchart et al.*, 2006]. The upwelling covers a broad latitude range from around −30°S to 30°N and regions poleward of 30° are marked mainly by downwelling. It should be pointed out that there are also rising branches of $\bar{\omega}'$ at midlatitudes. A similar feature has been noted in previous studies [*Edmon et al.*, 1980, 1981; *Butchart et al.*, 2006] and this can be largely accounted for in terms of latent heat released at low levels and then transported upward (in the Eulerian sense) by the midlatitude baroclinic disturbances [*Simmons and Hoskins*, 1978]. However, $\bar{\omega}'$ averaged poleward of 30° is positive in all experiments implying that the net effect of the BD
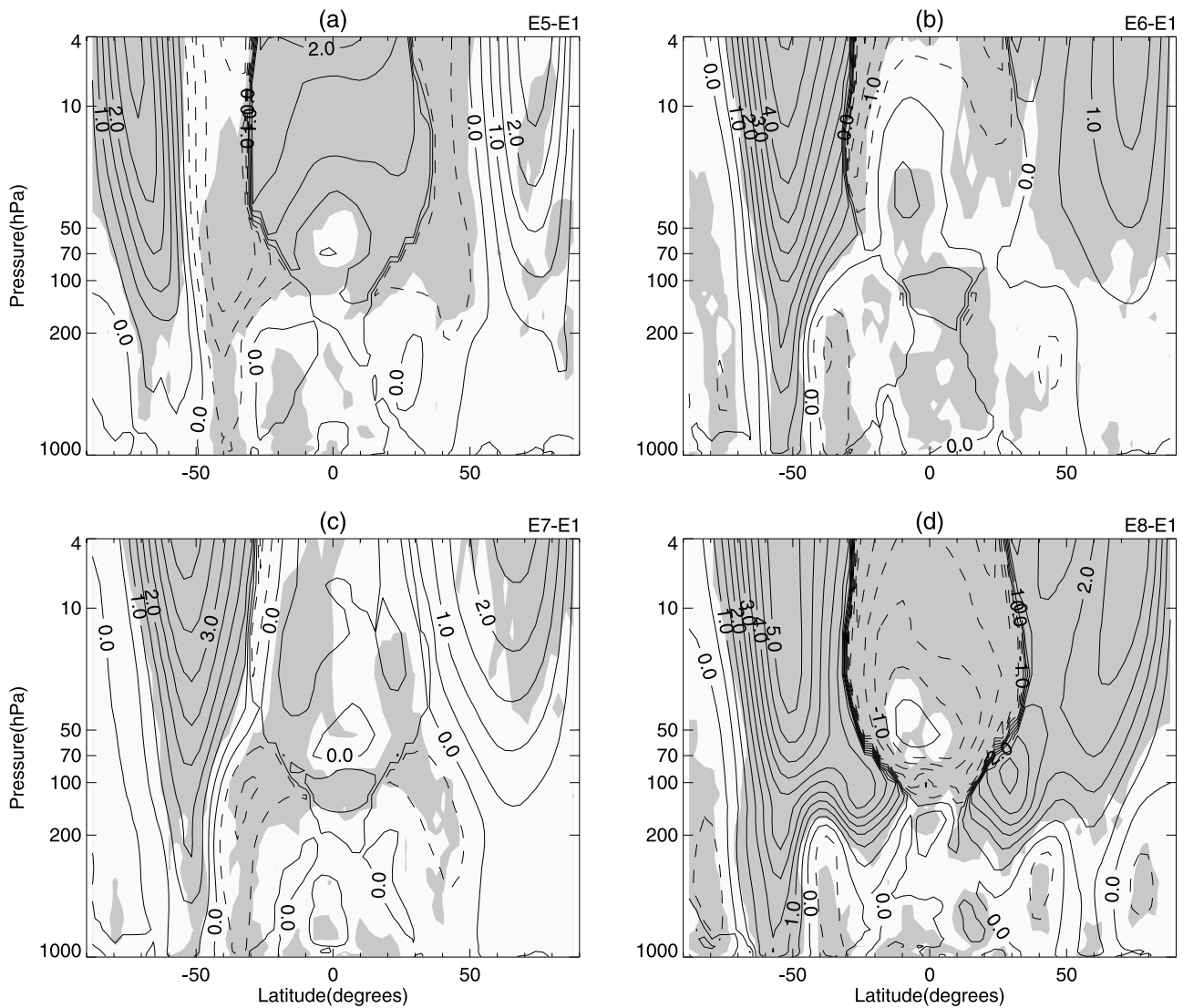
Figure 5. Latitude-pressure cross sections of zonal mean zonal wind differences (m s^{-1}) between (a) experiments E5 and E1, (b) E6 and E1, (c) E7 and E1, and (d) E8 and E1. Differences significant at 95% confidence level are shaded. Solid lines represent positive values, and dashed lines represent negative values. Contour interval is 0.5 m s^{-1}.

circulation from middle to high latitudes will cause a downward mass transport. It should be pointed out that the rising branch in $\bar{\omega}'$ should not occur in Lagrangian-mean meridional circulation. However, *Butchart et al.* [2006] compared several models (some of them also having a rising branch in the BD circulation) and found that all models can reproduce the observed upwelling across the tropical tropopause balanced by downwelling in the extratropics.

[20] Figure 7 shows the width of the "turnaround latitudes" [*Butchart and Scaife*, 2001], where circulation changes from upward to downward near tropics at the 100 hPa model level. The average width of the turnaround latitudes at 100 hPa in experiments E5, E7 and E9 are 47.2°, 47.4° and 47.2°, respectively, and is 46.1° in the control experiment E1, implying that warming of the whole atmosphere or the UTLS region tends to widen the region with upward motions in the tropics. A maximum 1.3° increase in the width of the turnaround latitudes can be caused by a

global 15% ozone increase together with CO_2 doubling. Further examination of the width of the turnaround latitudes near the tropics at 85 and 70 hPa levels shows a similar feature. Note that differences in the width of turnaround latitudes between the control experiment E1 and other experiments are significant above 90% confident level (Student-T test) except for experiment E2. It appears that a significant warming of the stratosphere tends to widen the tropical upwelling region. It is interesting that the average turnaround latitudes in experiment E8 is smaller than the control experiment E1. By looking at Figure 3 and Figure 7 together, we can see that the significant warming of the UTLS (in experiments E5, E7, E9) tends to increase the width of turnaround latitudes. In contrast, the significant warming below 100 hPa and cooling just above 100 hPa (Figure 3g) is associated with a decrease in the width of turnaround latitudes in Figure 7g.
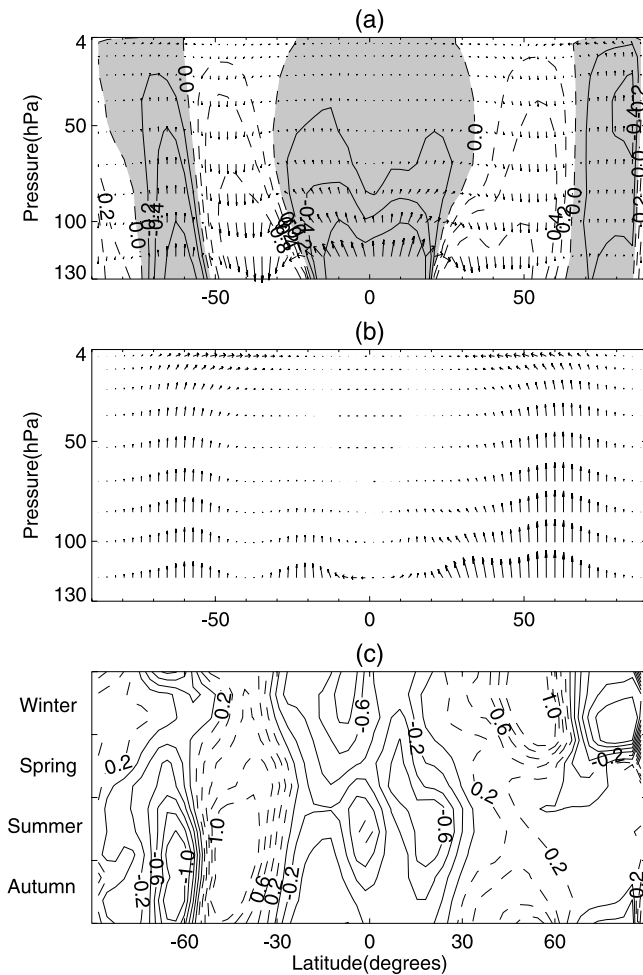
Figure 6. (a) BD circulation vectors, (b) EP flux vectors, and (c) the annual cycle of vertical velocity of the BD circulation diagnosed from the control experiment E1. Regions with upward motions are shaded in Figure 6a. Contour lines represent the vertical velocity field with solid lines denoting upward motion and dashed lines denoting downward motion. Contour interval is 0.2 Pa/s × 1000 in Figures 6a and 6c.

[21] Figure 8 shows profiles of $\bar{\omega}'$ averaged between the turnaround latitudes near the tropics for four different seasons. Note that in spring (MAM) and summer (JJA) a 15% decrease in O_3 (E2 and E3) leads to an increase in $\bar{\omega}'$ in this region, implying increased tropical upwelling (Figures 8a and 8b). In fall (SON) and winter (DJF), 15% O_3 decreases cause no significant changes in $\bar{\omega}'$ (Figures 8c and 8d). In all experiments with a 15% O_3 increase (E4, E5, E7, and E9) the tropical upwelling in all four seasons tends to be weakened compared to the control experiment E1. The $\bar{\omega}'$ responses to CO_2 doubling with (E8) and without (E6) SST change are different. In experiment E8 $\bar{\omega}'$ increases significantly while in experiment E6 $\bar{\omega}'$ decreases. These results are qualitatively consistent with previous findings of the effect of increasing GHGs on STE [e.g., *Butchart and Scaife*, 2001; *Read et al.*, 2001; *Austin and Li*, 2006]. Previous studies have also shown that the BD circulation is significantly strengthened in a doubled CO_2 climate. *Kodama et al.* [2007] found SST changes due to increased

CO_2 produce a more significant effect on the BD circulation than CO_2-induced radiation changes in the atmosphere. Figure 8 clearly shows that the doubling of CO_2 together with SST associated changes gives rise to a significant increase in the tropical upwelling. Figure 8 also suggests that the $2xCO_2$-induced warming in the atmosphere can even cause a decrease in the BD circulation. Also noticeable is that a 15% increase in ozone between 200 and 70 hPa (E9) causes an even more significant effect on $\bar{\omega}'$ between the turnaround latitudes than a 15% global ozone increase (E5) (see Figures 8c and 8d), suggesting that ozone changes in the UTLS region have a more significant impact on the STE than ozone changes elsewhere.

[22] A more quantitative measure of the effect of changing ozone layer on the STE can be gained from the cross-tropopause mass flux associated with the BD circulation. Following *Austin et al.* [2003], the upward mass flux is calculated at the 100 hPa model as the difference in the mass stream function F_m between the turnaround latitudes near the tropics. The residual mean stream function ψ is defined by

$$\partial\psi/\partial\phi = -a\cos\phi\bar{\omega}', \quad \partial\psi/\partial p = \cos\phi\bar{v}',$$

where $(\bar{v}', \bar{\omega}')$ is the residual mean meridional circulation and a is the radius of the Earth. The mass stream function F_m is defined as $F_m = 2\pi a\psi/g$. Integrating the above equations between the turnaround latitudes, we can get the upward mass flux at a given level.

[23] Table 2 presents the tropical upward mass flux at the 100 hPa model level in different experiments. The mass fluxes integrated poleward from the turnaround latitudes in both the hemisphere are also listed. We can see from Table 2 that a global 15% O_3 decrease or a 15% O_3 decrease above 100 hPa can cause an increase of about 7.2% or 4.6% in the tropical upward mass flux at 100 hPa. The changes in the topical upward flux in experiments E4 (15% increase of ozone below 100 hPa) and E6 (CO_2 doubling) are relatively small. A global 15% O_3 increase causes a decrease in tropical upward mass flux by 4.0% while CO_2 doubling and a global 15% O_3 increase together also lead to 4.0% decrease in the tropical upward mass flux. These results indicate that the warming caused by O_3 increases tends to decrease tropical upward flux while the cooling tends to increase the tropical upward flux. *Rind et al.* [2001] estimated a 30% increase in STE mass flux due to a doubling of CO_2 concentrations which is much larger than our estimate from experiment E6. As mentioned above, without considering SST changes, the doubling of CO_2 in the model's radiation scheme cannot cause a significant change in the BD circulation. If the SST changes are considered, doubling of CO_2 results in a 20.4% increase in the tropical mass flux at 100 hPa which is close to previous findings. Consistent with Figure 8, the change of the tropical mass flux at 100 hPa in experiment E9 (5.6%) is even bigger than in experiment E5 (4.0%) suggesting the importance of ozone changes in the UTLS region in modulating the STE.

[24] The mass fluxes at middle and high latitudes are downward in both hemispheres. The downward mass flux in the northern hemisphere is overall larger than that in the southern hemisphere in all eight experiments. The hemi-
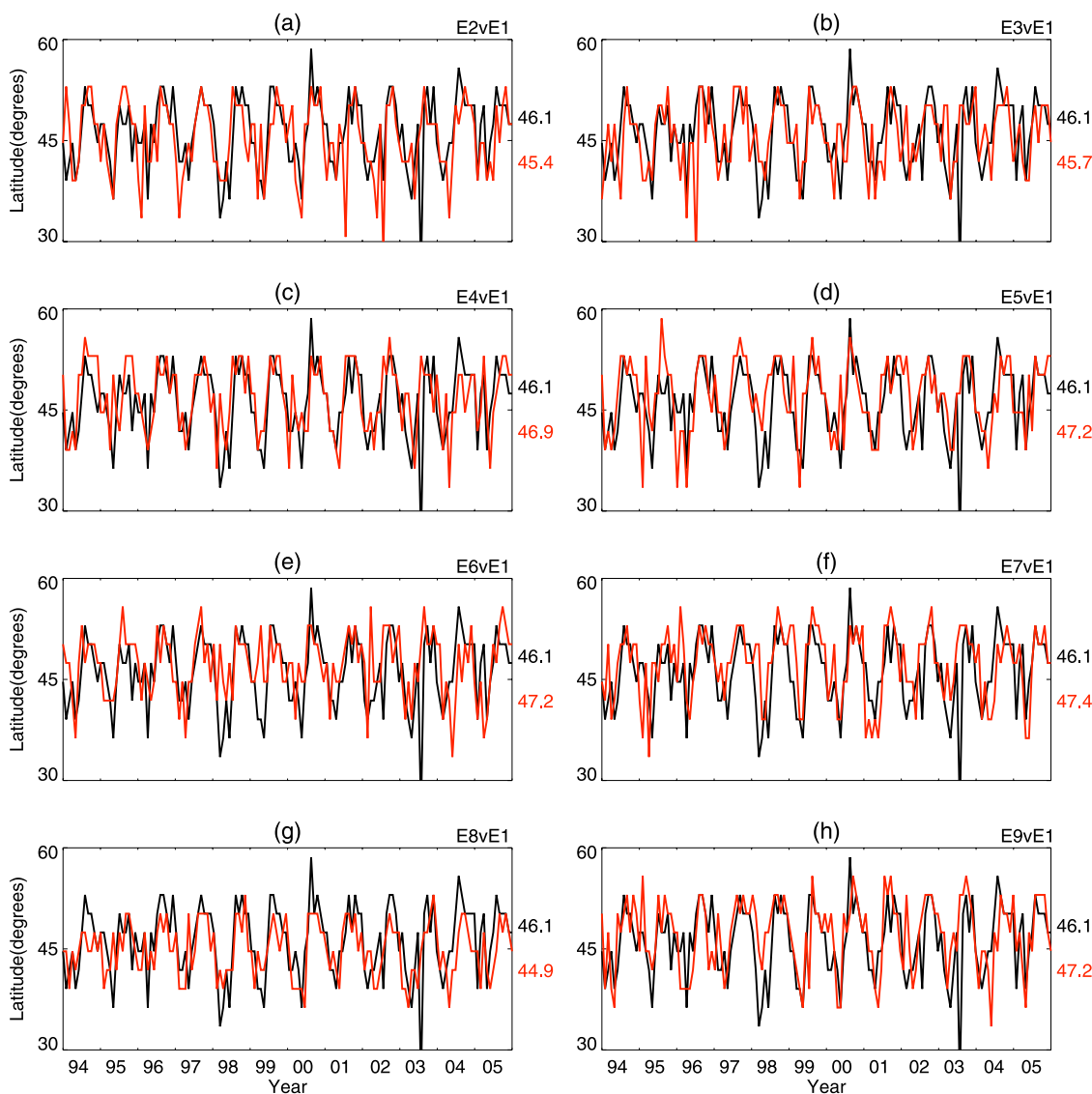
Figure 7. Time series of the width (degrees latitude) of the turnaround latitudes (red lines) in experiment (a) E2, (b) E3, (c) E4, (d) E5, (e) E6, (f) E7, (g) E8, and (h) E9. The corresponding time series for the control experiment E1 (black lines) is also given for reference in each panel. The mean of each time series is marked on the right side of each panel.

sphere difference in the mass flux is relatively large in the doubled CO_2 experiment E6 and E8 and smallest in experiment E5 (a global 15% increase in O_3). *Schoeberl* [2004] showed that the STE mass flux at the southern hemisphere extratropics is only half as large as that at the northern hemisphere extratropics. The hemispheric differences in the downward mass flux in Table 2 are not as significant as those of *Schoeberl* [2004], possibly owing to different levels and approaches in estimating the mass flux.

5. Effects on Stratospheric Water Vapor

[25] Here we examine the effect of changing ozone on the transport of the atmospheric water vapor from the troposphere to stratosphere. It should be noted that the water vapor transport in a low-vertical resolution model with an Eulerian dynamical core is not expected to be very accurate. However, Figure 1 shows that the magnitudes of modeled

water vapor in the UTLS region are similar to those in the UM run. Moreover, our results are interpreted in terms of water vapor differences between a sensitivity run and the control run which are mainly caused by changes in temperature and transport near the troposphere. Therefore, even if the stratospheric water vapor is not accurately predicted by the model, some insights on the effects STE changes on water vapor can still be obtained. Figure 9 shows the time variations of the stratospheric water vapor in different experiments. Compared to the control experiment E1, the water vapor mixing ratios in E2 and E3 are decreased significantly within the 30°N−30°S and 30°N−90°N latitude bands owing to the cooling effect of a 15% O_3 decrease above 100 hPa. Note that there are no significant differences in water vapor between experiment E3 (a 15% decrease of ozone above 100 hPa) and E2 (a global decrease of O_3 by 15%) implying that a 15% O_3 decrease below 100 hPa has no significant impact on the water vapor entering the
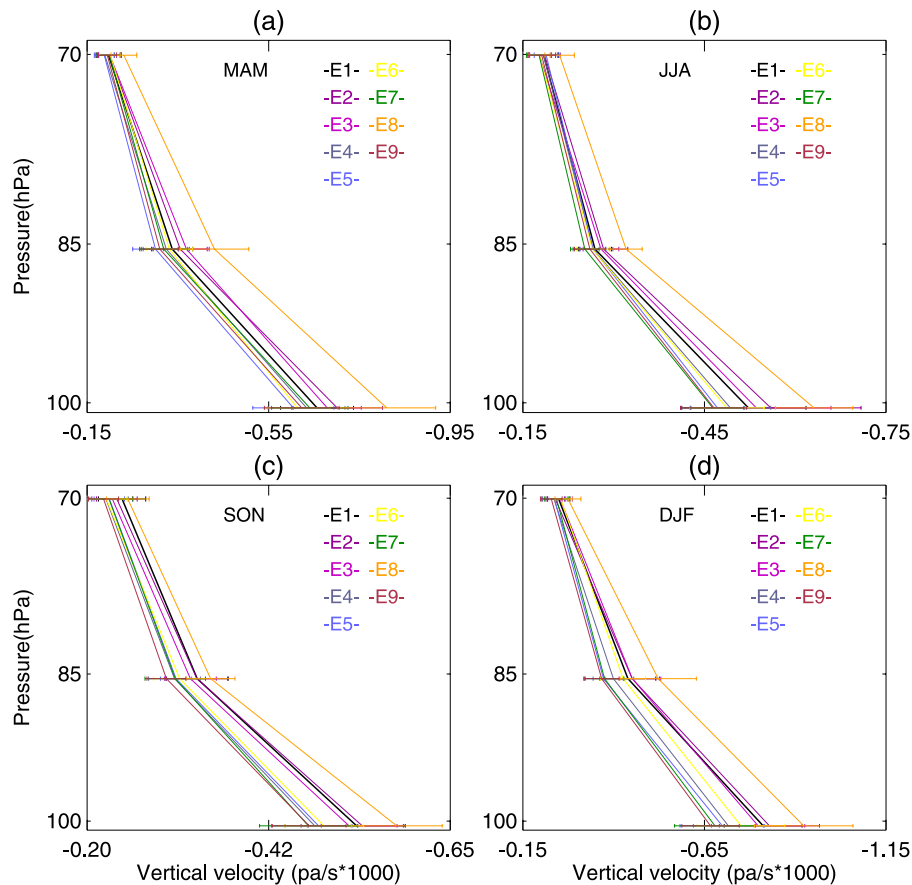
Figure 8. Profiles of $\overline{\omega}$ averaged between turnaround latitudes near the tropics for four different seasons. Lines with different colors represent different experiments. Error bars showing variability (1 standard deviation of each time series) are included on the profiles.

stratosphere. Water vapor in experiments E4 and E5 is obviously higher than in the control experiment E1 owing to warming effects of increased ozone. It is evident that a 15% increase of ozone below 100 hPa allows more water vapor to enter the stratosphere owing to the warming of the upper troposphere while a 15% decrease of ozone above 100 hPa causes less water vapor in the stratosphere owing to the cooling of the lower stratosphere.

[26] Figure 9f shows that the water vapor in experiment E6 is nearly the same as that in the control experiment E1. It is interesting that the significant cooling of the stratosphere by 2xCO$_2$ causes no significant change in stratospheric water vapor. However, stratospheric water vapor is significantly increased in the doubled CO$_2$ experiment with SST changes (Figures 9h), suggesting that doubled CO$_2$-induced SST changes have a more profound impact on the stratospheric water vapor than the 2xCO$_2$-induced radiative cooling and warming in the atmosphere. The water vapor in experiment E7 has the same magnitude as that in experiments E5 and E8, further confirming that the warming induced by a 15% ozone increase and 2xCO$_2$-induced SST changes have a more significant effect on the stratospheric water than 2xCO$_2$-induced cooling and warming in the atmosphere only. The water vapor in experiment E9 is slightly lower than that in E5 but is still much larger than in the control experiment E1.

[27] An important feature of the water vapor in the lower stratosphere is the so-called "tape recorder" [e.g., *Mote et al.*, 1996; *Randel et al.*, 2001]. A similar tape recorder type signal can be seen in Figure 9 within the latitude band of 30°N−30°S, although the amplitude of the signal looks different between the experiments. To examine the extent to which the amplitude of the tape recorder is affected by ozone changes, Figure 10 shows the changes in the amplitude of the stratospheric water vapor tape recorder calculated using a Fourier transform method. We can see that a 15% O$_3$ decrease causes a significant decrease in the amplitude

Table 2. Mass Flux at 100-hPa Level in Different Experiments[a]

Experiment	SH Downwelling	Tropics Upwelling	NH Downwelling
E1	−7.44	15.27	−7.84
E2	−7.94(+6.8%)	16.32(+7.2%)	−8.42(+7.7%)
E3	−7.73(+4.1%)	15.91(+4.6%)	−8.21(+5.1%)
E4	−7.27(−2.7%)	14.92(−2.0%)	−7.66(−2.6%)
E5	−7.25(−2.7%)	14.58(−4.0%)	−7.36(−6.4%)
E6	−7.29(−1.4%)	15.27(0.0%)	−8.02(+2.6%)
E7	−7.08(−4.1%)	14.62(−4.0%)	−7.66(−2.6%)
E8	−8.72(+17.6%)	18.27(+20.4%)	−9.30(+20.5%)
E9	−7.09(−4.7%)	14.42(−5.6%)	−7.39(−5.7%)

[a]Negative values represent downward mass flux, positive values denote upward mass flux. The mass flux is in units of 10^9 kg/s. Percentage changes of the mass flux (in parentheses) caused by ozone changes in different experiments are estimated relative to that of the control experiment E1.
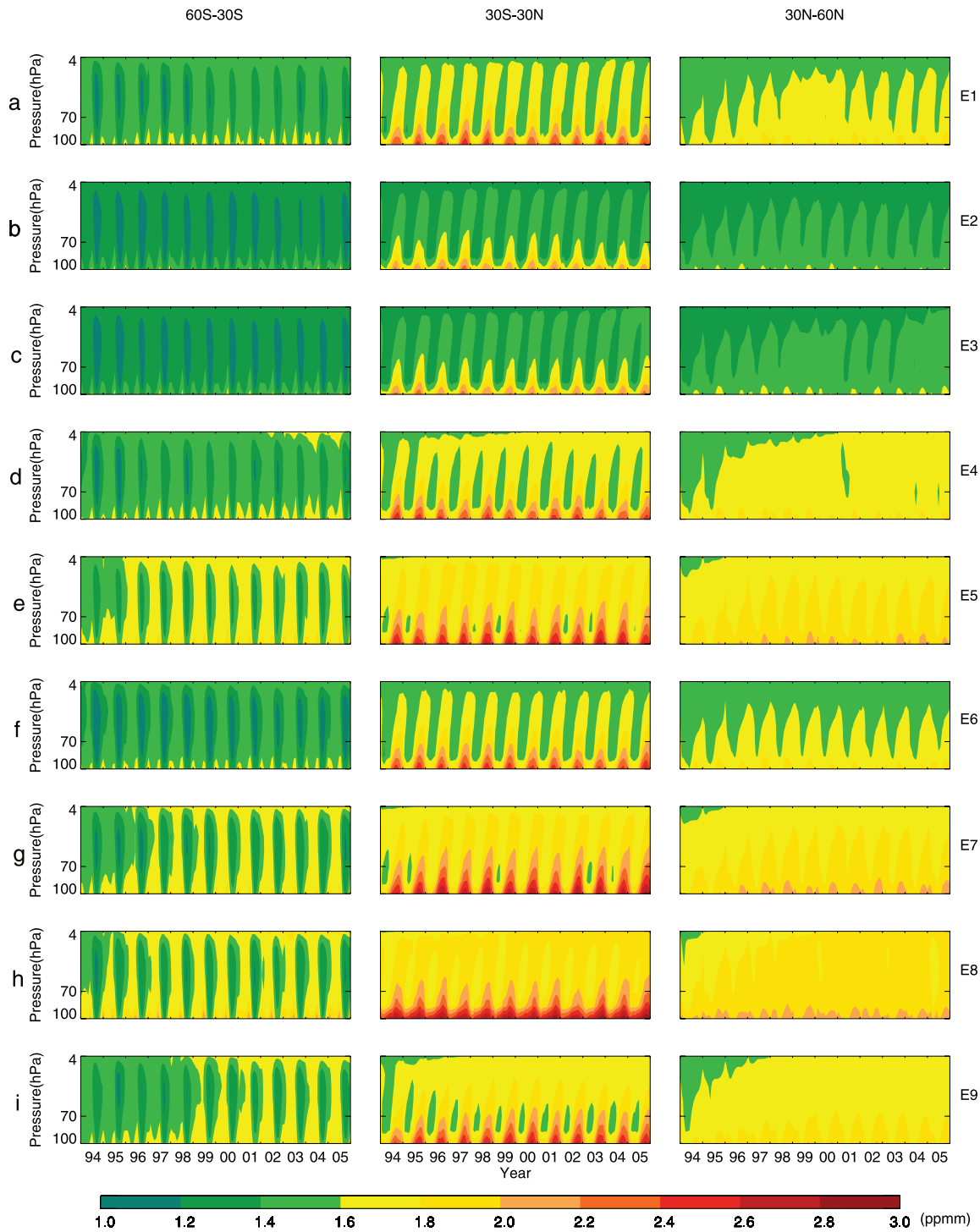
Figure 9. Zonal mean water vapor fields in the stratosphere (ppmm) averaged over different latitude bands in different experiments. The corresponding experiment names are marked on the right side of each row.

compared to that of the control experiment E1 (Figures 10a and 10b), particularly in the tropical UTLS region with a maximum decrease of 80 ppb. A 15% increase of ozone below 100 hPa or a 15% global increase of ozone causes no statistically significant change in the amplitude in the tropical UTLS region (not shown), recalling that a 15% increase of ozone below 100 hPa tends to cause a cooling in the stratosphere. Overall, a stratospheric cooling tends to

cause a decrease in the amplitude of the stratospheric water vapor while the warming of the troposphere allows more water vapor to enter the stratosphere. It is interesting that the amplitude of the water vapor signal in experiment E7 is increased significantly in the tropical stratosphere compared to that in the control experiment E1 (Figure 10c). This result suggests that significant warming of the UTLS region (see Figure 3f) due to a global 15% O_3 increase and CO_2
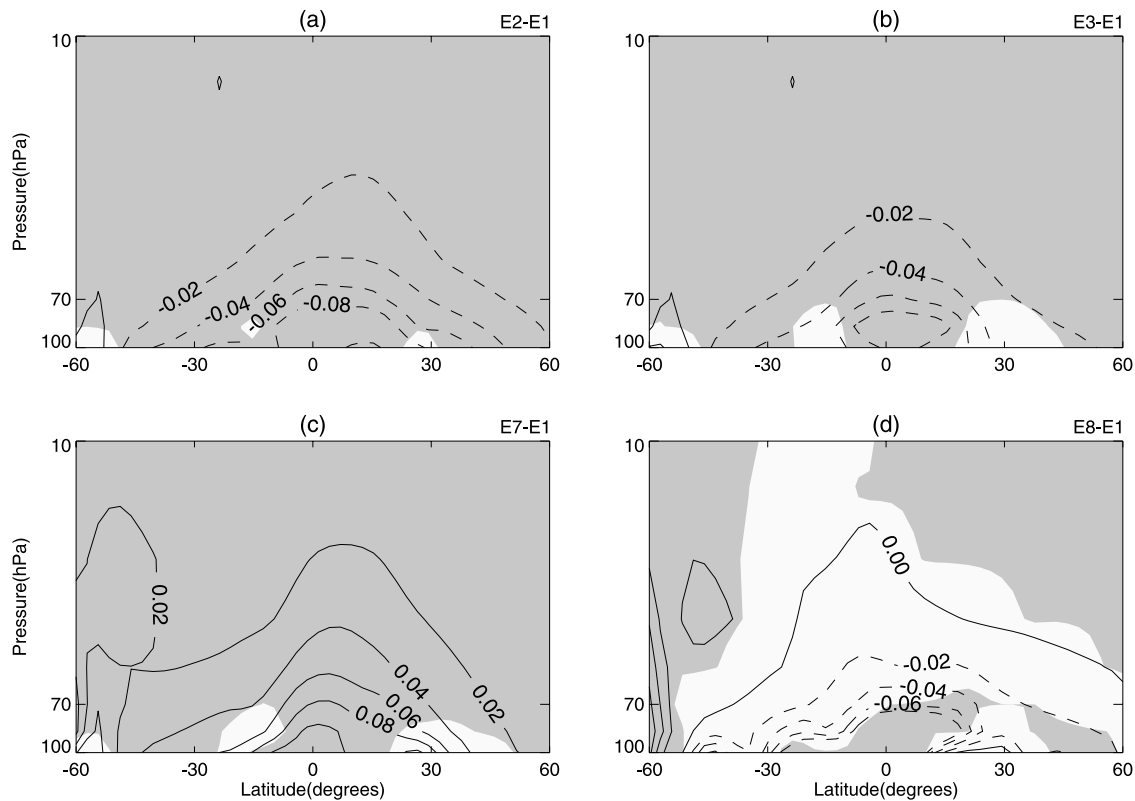
Figure 10. Differences in the amplitudes of the tape recorder signals in stratospheric water vapor between (a) experiments E2 and E1, (b) E3 and E1, (c) E7 and E1, and (d) E8 and E1. Contour interval is 0.02 ppmm. Differences significant at the 95% confidence level are shaded. (This significant test computes the F-statistic and tests the probability that two sample populations X and Y have significantly different variances.)

doubling can increase the amplitude of the stratosphere water vapor. In experiment E8 (Figure 10d), $2 \times CO_2$ causes a significant cooling in the stratosphere which may tend to decrease the amplitude of the stratosphere water vapor signal. However, significant warming in the troposphere due to CO_2 doubling together with SST feedbacks tends to increase the amplitude. The integrated effect of CO_2 doubling is to decrease the amplitude of water vapor in the lower stratosphere.

[28] It is well known that the water vapor entering the stratosphere is mainly controlled by the temperature near the tropical tropopause. *Tian and Chipperfield* [2006] used a CCM to simulate the stratospheric water vapor trend for the period 1979 to 2020 and found that the temperature change at 100 hPa causes up to 70% of the model lower stratospheric water vapor change when methane oxidation processes are not considered. To better understand the stratospheric water vapor changes caused by ozone changes, it is necessary to examine the modulation of the tropopause height and tropopause temperatures resulting from them.

[29] Figure 11 shows the zonal and annual mean thermal tropopause (WMO definition) and the cold point tropopause between 30°S and 30°N. The thermal tropopause climatology for the time period of 1994–2005 from NCEP reanalysis data is also plotted for reference. Compared to the NCEP thermal tropopause climatology, the modeled thermal tropopause is slightly higher, possibly owing to the coarse model vertical resolution and pressure-height conversion.

Figure 11 indicates that a global 15% O_3 decrease results in a higher tropopause while a global 15% O_3 increase results in a lower tropopause relative to that of the control experiment E1. The thermal tropopause height in experiment E3 (15% decrease in ozone above 100 hPa) is nearly the same as that in E2 (a global 15% O_3 decrease). However, the cold point tropopause in experiment E3 is higher than that in E2. A 15% increase in O_3 below 100 hPa (E4) gives no significant change in tropopause height compared with that of the control experiment E1. The cold point tropopause in experiment E7 is the lowest, owing to combined warming effects of the O_3 increase and doubling of CO_2. Also noticeable is that the tropical tropopause height in the double CO_2 experiment without SST changes (E6) is nearly the same as that in the control experiment E1. In contrast, the tropical tropopause height in the doubled CO_2 experiment with SST changes (E8) is the highest among all experiments possibly owing to stronger convective activities caused by the SST changes in experiment E8. As expected, the tropopause in experiment E9 is close to that in experiment E5.

[30] Figure 12 shows the annual cycle of tropical (30°S−30°N) thermal and cold point tropopause temperature and anomalies about the annual mean. The tropopause temperature and its anomalies have a similar annual cycle in all experiments with the lowest tropopause temperature and anomalies from January to March and the highest from July to October. Consistent with the tropopause height in Figure
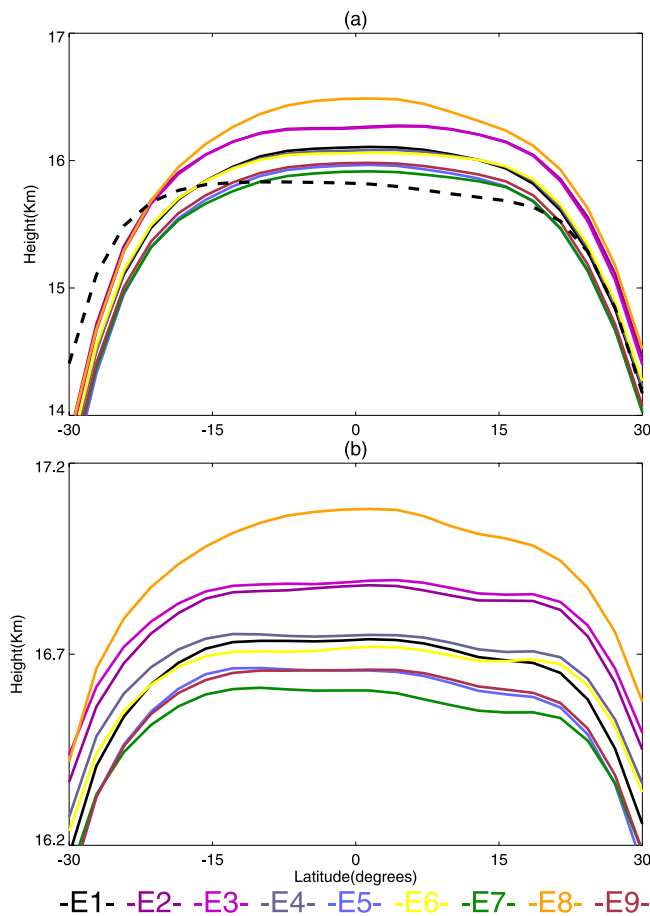
Figure 11. Zonal and annual mean (a) thermal tropopause (WMO definition) and (b) cold point tropopause climatologies within the 30°S−30°N latitude band. The dashed line in Figure 11a is the NCEP thermal tropopause climatology for the period from 1994 to 2005.

11, both the thermal and cold point tropopause temperatures in E2 and E3 are the lowest corresponding to higher tropical tropopause heights in Figure 11, while a global 15% O_3 increase (E5 and E7) gives the highest tropopause temperatures. The tropical tropopause temperatures and their anomalies about the annual mean are quite different. The doubling of CO_2 without SST changes (E6) has no significant effect on the tropopause temperature and tropical tropopause height, consequently the stratospheric water vapor in experiment E6 has nearly the same magnitude as that in the control experiment E1 (Figure 9). However, the doubling of CO_2 with SST changes (E8) gives the highest tropical tropopause height and higher tropopause temperatures relative to the control experiment E1. Also note that the amplitude of the temperature anomalies in experiment E8 is the smallest among the experiments.

[31] By considering Figures 9, 11 and 12 together, we can see that lowest tropopause temperatures correspond to the lowest stratospheric water vapor (experiment E2 and E3) while the highest tropopause temperature results in highest stratospheric water vapor (experiment E5 and E7, E8, and E9). However, the highest tropical tropopause height does not necessarily correspond to a lowest tropopause temper-

ature and stratospheric water vapor as is evident in experiment E8. From Figure 3 we noted that a 15% increase of O_3 below 100 hPa causes a slight cooling in the stratosphere and is supposed to be related to increased stratospheric water vapor. Figure 9 indicates that the stratospheric water vapor in experiment E4 (15% increase of O_3 below 100 hPa) is indeed slightly higher than that in the control experiment E1. However, from Figure 12 we can see that the tropopause temperature in experiment E4 is also slightly higher than that in the control experiment E1 from January to March, suggesting that more water vapor enters the stratosphere in winter in experiment E4. Figure 11 indicates that the cold point tropopause height in experiment E4 is slightly higher than that in the control experiment E1 implying that convective motions reach a higher altitude in a warming troposphere. Note that the tropopause heights in the experiments with a warming of the whole atmosphere or the UTLS (E5, E7, and E9) are much lower than that in the control experiment E1.

6. Summary and Conclusions

[32] Using the CAM3 general circulation model a series of time-slice runs have been performed to examine the radiative effects of prescribed atmospheric ozone changes on STE processes. Different ozone change scenarios have been imposed in the model to investigate the effects of an arbitrary 15% O_3 change on the temperature, BD circulation and associated cross-tropopause mass flux, as well as the water vapor entering the stratosphere.

[33] We find that a 15% global O_3 increase causes a maximum cooling of 2.4 K in the stratosphere and a ∼7% increase in tropical upwelling, while a 15% global O_3 increase causes a maximum 2.1 K warming in the stratosphere and a ∼4% decrease in tropical upwelling. Water vapor entering the stratosphere is controlled mainly by the tropopause temperature and so a global 15% O_3 decrease/increase, resulting in a higher/lower tropical tropopause and lower/higher tropopause temperatures, causes less/more stratospheric water vapor and a smaller/larger amplitude of the tape recorder signal. The effect of a 15% change of O_3 below 100 hPa is relatively small. However, changes of O_3 below 100 hPa can also modify stratospheric water vapor by altering the tropopause temperatures. The effect of O_3 changes on the turnaround latitudes, where circulation changes from upward to downward near the tropics, is not very significant. However, it is found that a global 15% O_3 increase tends to increase the width of the turnaround latitudes and that the warming of UTLS region has a more significant impact on the turnaround latitudes than the tropospheric warming only. The issue merits further investigation. A further test of imposed ozone changes between 200 and 70 hPa indicates that a 15% ozone increase in the UTLS region has similar effects on the STE processes as those of a global 15% ozone increase implying that ozone changes in the UTLS region are most important for this process.

[34] SST changes caused by increasing GHGs in the atmosphere have a significant impact on STE processes. Without the corresponding SST changes from the CO_2 doubling in the model, the radiative effects of the CO_2 doubling only cannot generate significant changes in the
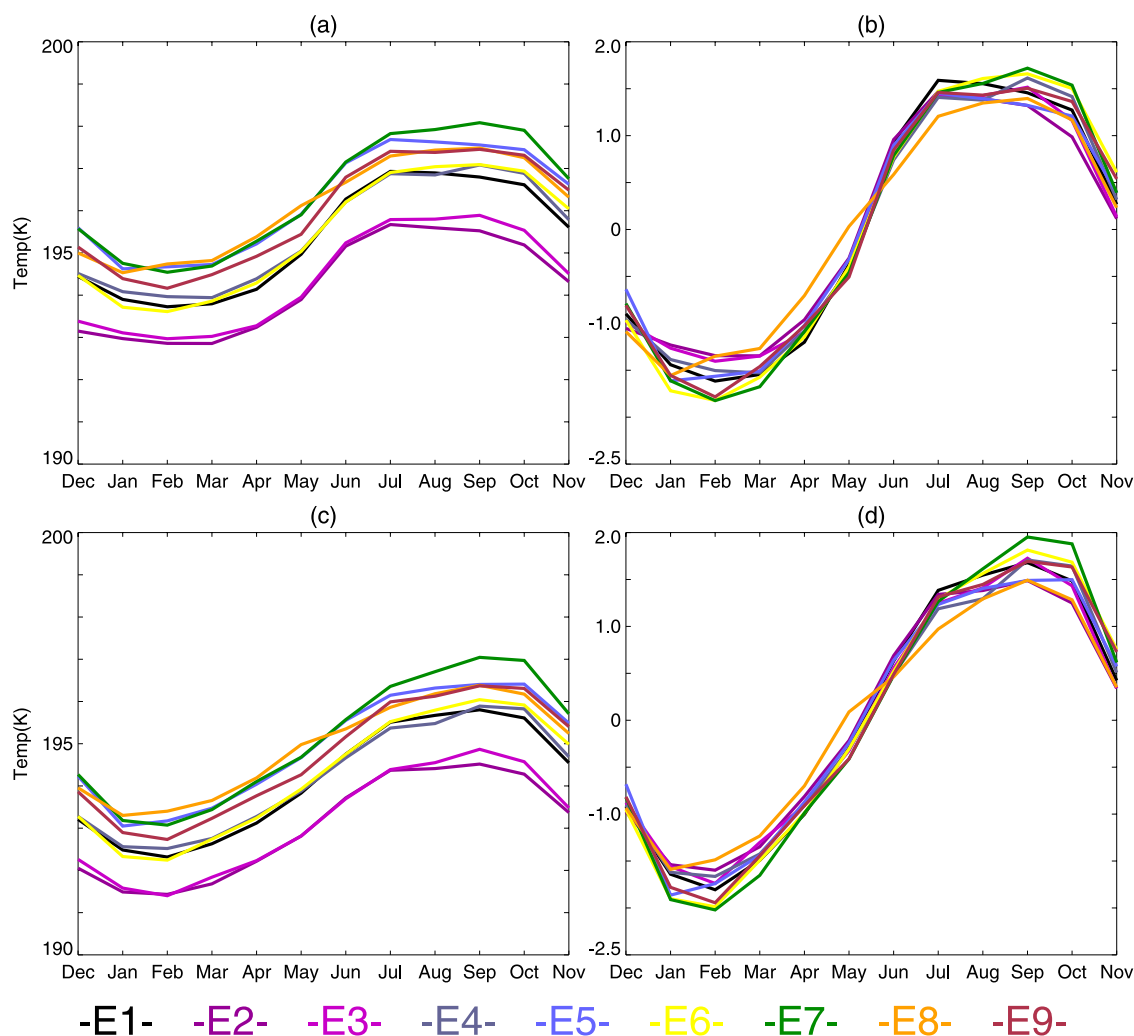
Figure 12. Annual cycle of tropical (30°S−30°N) (a) thermal and (c) cold point tropopause temperatures (K). The corresponding (b) thermal and (d) cold point tropopause temperature anomalies about the annual mean are also shown.

tropopause height and cross tropopause mass flux found in the previous studies. The effect of CO_2 doubling is even less significant than a global 15% O_3 increase without the SST responses. When the SST changes are considered in the doubled CO_2 experiment, the tropical upwelling is increased by 20.4%, which is in agreement with previous findings. It is also found that $2\times CO_2$ with SST changes significantly increases the tropopause height owing to more and stronger convective activities over warmer oceans, However, significant warming of the troposphere prevents the tropopause temperature decreasing significantly in a doubled CO_2 climate.

References

Austin, J., and F. Li (2006), On the relationship between the strength of the Brewer-Dobson circulation and the age of stratospheric air, *Geophys. Res. Lett.*, *33*, L17807, doi:10.1029/2006GL026867.

Austin, J., et al. (2003), Uncertainties and assessments of chemistry-climate models of the stratosphere, *Atmos. Chem. Phys.*, *3*, 1−27.

Boville, B. A., P. J. Rasch, J. J. Hack, and J. R. McCaa (2006), Representation of clouds and precipitation processes in the Community Atmosphere Model version 3 (CAM3), *J. Clim.*, *19*, 2184−2198, doi:10.1175/JCLI3749.1.

Butchart, N., and A. A. Scaife (2001), Removal of chlorofluorocarbons by increased mass exchange between the stratosphere and troposphere in a changing climate, *Nature*, *410*, 799−802, doi:10.1038/35071047.

Butchart, N., J. Austin, J. R. Knight, A. A. Scaife, and M. L. Gallani (2000), The response of the stratospheric climate to projected changes in the concentrations of well-mixed greenhouse gases from 1992 to 2051, *J. Clim.*, *13*, 2142−2159, doi:10.1175/1520-0442(2000)013<2142:TROTSC>2.0.CO;2.

Butchart, N., et al. (2006), Simulations of anthropogenic change in the strength of the Brewer-Dobson circulation, *Clim. Dyn.*, *27*, 727−741, doi:10.1007/s00382-006-0162-4.

Chipperfield, M. P., and W. Feng (2003), Comment on "Stratospheric Ozone Depletion at northern mid-latitudes in the 21st century: The importance of future concentrations of greenhouse gases nitrous oxide and methane", *Geophys. Res. Lett.*, *30*(7), 1389, doi:10.1029/2002GL016353.

Collins, W. D., et al. (2004), Description of the NCAR Community Atmosphere Model (CAM3), *Tech. Rep. NCAR/TN-464_STR*, 226 pp., Natl. Cent. for Atmos. Res., Boulder, Colo.

Collins, W. D., P. J. Rasch, B. A. Boville, J. J. Hack, J. R. McCaa, D. L. Williamson, B. P. Briegleb, C. M. Bitz, S. J. Lin, and M. Zhang (2006), The formulation and atmospheric simulation of the community atmosphere model version 3 (CAM3), *J. Clim.*, *19*, 2144−2161, doi:10.1175/JCLI3760.1.

Collins, W. J., R. G. Derwent, B. Gamier, C. E. Johnson, M. G. Sanderson, and D. S. Stevenson (2003), Effect of stratosphere-troposphere exchange

on the future tropospheric ozone trend, *J. Geophys. Res.*, *108*(D12), 8528, doi:10.1029/2002JD002617.

Dameris, M., C. Schnadt, and F. Mager (2002), Future changes of stratospheric dynamics due to chemistry-climate interaction, paper presented at XXVII General Assembly, Eur. Geophys. Soc., Nice, France.

Edmon, H. J., B. J. Hoskins, and M. E. McIntyre (1980), Eliassen-Palm cross-sections for the troposphere, *J. Atmos. Sci.*, *37*, 2600–2616.

Edmon, H. J., B. J. Hoskins, and M. E. McIntyre (1981), Corrigendum, *J. Atmos. Sci.*, *38*, 1115.

Eyring, V., et al. (2007), Multimodel projections of stratospheric ozone in the 21st century, *J. Geophys. Res.*, *112*, D16303, doi:10.1029/2006JD008332.

Farman, J. G., B. G. Gardiner, and J. D. Shanklin (1985), Large losses of total ozone in Antarctica reveal seasonal ClO$_x$/NO$_x$ interaction, *Nature*, *315*, 207–210, doi:10.1038/315207a0.

Fioletov, V. E., D. W. Tarasick, and I. Petropavlovskikh (2006), Estimating ozone variability and instrument uncertainties from SBUV(/2), ozonesonde, Umkehr, and SAGE II measurements: Short-term variations, *J. Geophys. Res.*, *111*, D02305, doi:10.1029/2005JD006340.

Forster, P. M. F., and K. Shine (1997), Radiative forcing and temperature trends from stratospheric ozone changes, *J. Geophys. Res.*, *102*(D9), 10,841–10,855, doi:10.1029/96JD03510.

Hansen, J., M. Sato, and R. Ruedy (1997), Radiative forcing and climate response, *J. Geophys. Res.*, *102*(D6), 6831–6864, doi:10.1029/96JD03436.

Holton, J. R., P. H. Haynes, M. E. McIntyre, A. R. Douglass, R. B. Rood, and L. L. Pfister (1995), Stratosphere-troposphere exchange, *Rev. Geophys.*, *33*, 403–439, doi:10.1029/95RG02097.

Hurrell, J. W., J. J. Hack, A. Phillips, J. Caron, and J. Yin (2006), The dynamical simulation of the Community Atmosphere Model Version 3 (CAM3), *J. Clim.*, *19*, 2162–2183, doi:10.1175/JCLI3762.1.

Intergovernmental Panel on Climate Change (2001), *Climate Change, The Scientific Basis. Contribution of Working Group I to the Third Assessment Report of the Intergovernmental Panel on Climate Change*, Cambridge Univ. Press, Cambridge, U.K.

Johnson, C. E., W. J. Collins, D. S. Stevenson, and R. G. Derwent (1999), Relative roles of climate and emissions changes on future tropospheric oxidant concentrations, *J. Geophys. Res.*, *104*(D15), 18,631–18,645, doi:10.1029/1999JD900204.

Karoly, D. J. (2003), Ozone and climate change, *Science*, *302*, 236–237, doi:10.1126/science.1090851.

Kodama, C., T. Iwasaki, K. Shibata, and S. Yukimot (2007), Changes in the stratospheric mean meridional circulation due to increased CO$_2$: Radiation- and sea-surface temperature–induced effects, *J. Geophys. Res.*, *112*, D16103, doi:10.1029/2006JD008219.

Mote, P. W., K. H. Rosenlof, M. E. Mcintyre, E. S. Carr, J. C. Gille, J. R. Holton, J. S. Kinnersley, H. C. Pumphrey, J. M. Russell, and J. W. Waters (1996), An atmospheric tape recorder: The imprint of tropical tropopause temperatures on stratospheric water vapor, *J. Geophys. Res.*, *101*(D2), 3989–4006, doi:10.1029/95JD03422.

Ramanathan, V., and R. E. Dickinson (1979), The role of stratospheric ozone in the zonal and seasonal radiative energy balance of the Earth-troposphere system, *J. Atmos. Sci.*, *36*, 1084–1104.

Randel, W. J., R. S. Stolarski, D. M. Cunnold, J. A. Logan, M. J. Newchurch, and J. M. Zawodny (1999), Trends in the vertical distribution of ozone, *Science*, *285*, 1689–1692.

Randel, W. J., F. Wu, A. Gettelman, J. M. Russell III, J. M. Zawodny, and S. J. Oltmans (2001), Seasonal variation of water vapor in the lower stratosphere observed in Halogen Occultation Experiment data, *J. Geophys. Res.*, *106*(D13), 14,313–14,326, doi:10.1029/2010JD900048.

Rayner, N. A., D. E. Parker, E. B. Horton, C. K. Folland, L. V. Alexander, D. P. Rowell, E. C. Kent, and A. Kaplan (2003), Global analyses of sea surface temperature, sea ice, and night marine air temperature since the late nineteenth century, *J. Geophys. Res.*, *108*(D14), 4407, doi:10.1029/2002JD002670.

Read, W. G., et al. (2001), UARS Microwave Limb Sounder upper tropospheric humidity measurement: Method and validation, *J. Geophys. Res.*, *106*(D23), 32,207–32,258, doi:10.1029/2000JD000122.

Reinsel, G. C., A. J. Miller, E. C. Weatherhead, L. E. Flynn, R. M. Nagatani, G. C. Tiao, and D. J. Wuebbles (2005), Trend analysis of total ozone data for turnaround and dynamical contributions, *J. Geophys. Res.*, *110*, D16306, doi:10.1029/2004JD004662.

Rind, D., J. Lerner, K. Shah, and R. Suozzo (1999), Use of on-line tracers as a diagnostic tool in general circulation model development: 2. Transport between the troposphere and stratosphere, *J. Geophys. Res.*, *104*(D8), 9151–9167, doi:10.1029/1999JD900006.

Rind, D., J. Lerner, and C. McLinden (2001), Changes of tracer distributions in the doubled CO$_2$ climate, *J. Geophys. Res.*, *106*(D22), 28,061–28,080, doi:10.1029/2001JD000439.

Roeckner, E., and M. Stendel (1999), Why is the global warming proceeding much slower than expected?, *J. Geophys. Res.*, *104*(D4), 3865–3876, doi:10.1029/1998JD200046.

Rosenfield, J. E., A. R. Douglass, and D. B. Considine (2002), The impact of increasing carbon dioxide on ozone recovery, *J. Geophys. Res.*, *107*(D6), 4049, doi:10.1029/2001JD000824.

Schoeberl, M. R. (2004), Extratropical stratosphere-troposphere mass exchange, *J. Geophys. Res.*, *109*, D13303, doi:10.1029/2004JD004525.

Schwarzkopf, M. D., and V. Ramaswamy (2002), Effects of changes in well-mixed gases and ozone on stratospheric seasonal temperatures, *Geophys. Res. Lett.*, *29*(24), 2184, doi:10.1029/2002GL015759.

Shindell, D. T., D. Rind, and P. Lonergan (1998), Increased polar stratospheric ozone losses and delayed eventual recovery owing to increasing greenhouse-gas concentrations, *Nature*, *392*, 589–592, doi:10.1038/33385.

Shindell, D. T., R. L. Miller, G. A. Schmidt, and L. Pandolfo (1999), Simulation of recent northern winter climate trends by greenhouse-gas forcing, *Nature*, *399*, 452–455, doi:10.1038/20905.

Shindell, D. T., G. A. Schmidt, R. L. Miller, and D. Rind (2001), Northern Hemisphere winter climate response to greenhouse gas, ozone, solar, and volcanic forcing, *J. Geophys. Res.*, *106*(D7), 7193–7210, doi:10.1029/2000JD900547.

Simmons, A. J., and B. J. Hoskins (1978), The life cycles of some nonlinear baroclinic waves, *J. Atmos. Sci.*, *35*, 414–432, doi:10.1175/1520-0469(1978)035<0414:TLCOSN>2.0.CO;2.

Stevenson, D. S., et al. (2006), Multimodel ensemble simulations of present-day and near-future tropospheric ozone, *J. Geophys. Res.*, *111*, D08301, doi:10.1029/2005JD006338.

Tett, S. F. B., J. F. B. Mitchell, D. E. Parker, and M. R. Allen (1996), Human influence on the atmospheric vertical temperature structure: Detection and observations, *Science*, *274*, 1170–1173, doi:10.1126/science.274.5290.1170.

Tian, W. S., and M. P. Chipperfield (2005), A new coupled chemistry-climate model for the stratosphere: The importance of coupling for future O$_3$-climate predictions, *Q. J. R. Meteorol. Soc.*, *131*, 281–303, doi:10.1256/qj.04.05.

Tian, W. S., and M. P. Chipperfield (2006), Stratospheric water vapor trends in a coupled chemistry-climate model, *Geophys. Res. Lett.*, *33*, L06819, doi:10.1029/2005GL024675.

Wang, W. C. (1985), Climatological effects of atmospheric ozone: A review, in *Atmospheric Ozone*, edited by C. S. Zerefos, pp. 98–102, D. Reidel, New York.

World Meteorological Organization (1999), Scientific assessment of ozone depletion: 1998, *Rep. 44*, Global Ozone Res. and Monit. Proj., Geneva.

World Meteorological Organization (2003), Scientific assessment of ozone depletion: 2002, *Rep. 47*, Global Ozone Res. and Monit. Proj., Geneva.

World Meteorological Organization (2007), Scientific assessment of ozone depletion: 2006, *Rep. 50*, Global Ozone Res. and Monit. Proj., Geneva.

———————————

M. P. Chipperfield, ICAS, School of Earth and Environment, University of Leeds, Leeds LS2 9JT, UK.

W. Tian and F. Xie, College of Atmospheric Sciences, Lanzhou University, Tianshui Road 222, Lanzhou, Gansu 730000, China. (wstian@lzu.edu.cn)